POLISH JOURNAL OF SOIL SCIENCE
VOL. LII/2 2019 PL ISSN 0079-2985

DOI: 10.17951/pjss/2019.52.2.295

RENATA KOŁODYŃSKA-GAWRYSIAK*, JERZY TRZCIŃSKI**,
MAŁGORZATA ZAREMBA***, PRZEMYSŁAW MROCZEK*

GRAIN-SIZE AND MICROSTRUCTURE OF THE LOESS FROM CLOSED DEPRESSIONS IN THE NAŁĘCZÓW PLATEAU (EAST POLAND)

Received: 25.04.2019
Accepted: 10.12.2019

Abstract. The investigation was conducted in the eastern part of the Nałęczów Plateau, a region of the Lublin Upland, in eastern Poland. The loess cover of this region was formed mainly during the last glaciation, and loess accumulation lasted until 15,000–12,000 BP. The undulating loess plateau with numerous oval-shaped closed depressions (CDs) is the main landform in the study area. Particle size distribution and SEM analyses were conducted for loess profiles under the bottoms and on the slopes of 4 CDs. Grain-size distribution characteristics as well as qualitative and quantitative micromorphological characteristics of the the loess forming the bottoms and slopes of the depressions were compared and discussed. It was documented that the differences between the loess forming the bottoms and slopes of the depressions are insignificant in the case of clay fraction content, but are considerable in the case of microstructure characteristics. The differences documented result from the impact of syn- and post-depositional diagenetic processes related mainly to suffosion and hydroconsolidation occurring under the influence of water. A quantitative assessment of the morphological effects of these processes was carried out in the context of the origin of closed depressions. The morphological effect of Holocene diagenetic processes was

* Faculty of Earth Sciences and Spatial Management, Maria Curie-Skłodowska University, Al. Kraśnicka 2CD, 20-718

** Wrocław Research Center EIT+, ul. Stabłowicka 147, 54-066 Wrocław

*** Institute of Archaeology, Faculty of Historical and Social Sciences, Cardinal Stefan Wyszyński University in Warsaw, ul. Wóycickiego 1/3, 01-938 Warsaw

manifested in the deepening of the initial closed depressions formed previously under the influence of primary morphogenetic processes.

Keywords: loess, grain-size distribution, quantitative analysis of microstructures, hydroconsolidation

1. INTRODUCTION

The loess cover of the Nałęczów Plateau consists of several loess patches of varying size, separated by river valleys where the loess cover is absent. The thickness of the loess cover varies both on the regional scale and within the individual patches. It reaches the maximum values in the western part and along the northern boundary of the region (up to 30 m). In the eastern part of the Nałęczów Plateau, the loess cover is usually 10 to 20 m thick (Harasimiuk 1987). The loess cover conceals small forms of the underlying sediments and mirrors the basic elements of their relief (Harasimiuk and Henkiel 1976). According to Maruszczak's (1991) stratigraphic scheme, the loess cover in the Nałęczów Plateau mainly consists of younger loess (LM) that accumulated during the Vistulian Glaciation from ca. 100,000 BP to 15,000/12,000 BP as well as, locally, of older upper loess (LSg) that accumulated during the Wartanian Glaciation (Saale 2) (210–135/130,000 BP). In terms of grain-size distribution, upper young loess (LMg) is characterised by a high silt fraction content (70–80%) and 10–15% clay fraction content and up to 10% calcium carbonate content (Harasimiuk 1987, Harasimiuk and Jezierski 2001).

Studies of the structure of sediments and sedimentary rocks may facilitate the recognition and interpretation of their origin as well as post-sedimentary alteration. The structure (microstructure in studies based on scanning electron microscopy – SEM) is defined as the sum of three components: 1) grain-size and mineral composition, and the chemical composition of the solid, liquid and gas phases, 2) fabric, referring to the distribution, shape and dimensions of grains and particles, and the character of the pore space, and 3) forces acting at the contacts between grains and particles (Mitchell 1993, Gillott 1987). The qualitative and quantitative description of microstructure is crucial, similarly to other parameters, in characterising geological-engineering properties. Such a complex approach to microstructural studies allows for a full recognition of sediment behaviour, particularly in macro-scale. This is extremely important in applied science.

The most exhaustive and detailed definition of loess microstructure was provided by Grabowska-Olszewska (1984, 1998). Aeolian loess is usually characterised by skeletal microstructure that usually developed in the form of a loose skeleton with evenly distributed pores. The grain skeleton is mainly composed of silty mineral grains, most frequently quartz grains. Clay particles and microaggregates are distributed unevenly and do not form a uniform continuous matrix. This material is most often concentrated on the surface of silt

grains in the form of membranes or on their contacts, forming various kinds of bonds, e.g. clay bridges binding skeleton grains together (Grabowska-Olszewska 1988). Contacts between structural elements are usually of a coagulation character, especially for non-weathered younger loess (Grabowska-Olszewska 1998). The orientation of structural elements does not occur. Pore space consists of evenly distributed open interaggregate and interparticle pores. The pores have various shapes, most often isometric, and their dimensions range from a fraction of a μm to 4–6 μm (Grabowska-Olszewska *et al*. 1984).

In non-weathered loess, structural elements are mainly connected with clay bonds, sensitive to the impact of water. In fully water-saturated loess, these bonds easily break, which leads to the destruction of the original structure of loess. Calcium carbonate occurs in the form of irregular concentrations on the surface of structural elements, connects grains and clay particles into aggregates and microagregates and creates mainly phase contacts. In weathered loess, water-resistant ferruginous and siliceous bonds occur. Loess with skeletal microstructure has varying sensitivity to water depending on the kind of structural bonds (Grabowska-Olszewska 1998). The infiltration of precipitation water into the ground mass built of loess triggers the movement of fine fractions and dissolution of salts, which causes the destruction of original loess microstructure caused by water infiltration (Liszkowski 1971, Frankowski and Grabowski 2006). The impermanence of loess structure is related to the unstable behavior of coagulation-based structural bonds that are quickly weakened and broken when exposed to water (Liszkowski 1971, Grabowska-Olszewska 1988).

Changes in loess microstructure under the influence of water are referred to as filtration-based consolidation (Liszkowski 1971) or hydroconsolidation (Rogers *et al*. 1994). The main factor triggering hydroconsolidation is the wetting of loess. The presence of carbonates and clay is the key element for the hydroconsolidation of loess (Smalley *et al*. 2006, Smalley and Markovic 2014). Changes in microstructure (e.g. disruption of the grain-bridging clay, rearrangement and closer stacking of the compact aggregate silt/clay peds) of loess result from saturation and may lead to the subsidence of loess.

The study objective is to assess degree of development and morphological effects of syn- and postdepositional diagenetic processes, resulted in changes of the loess features in closed depressions. The variation of the values of quantitative parameters of selected microstructural characteristics and loess grain-size distribution in the bottom and slopes of closed depressions were used for this purpose.

2. STUDY AREA

The investigation was conducted in the eastern part of the Nałęczów Plateau, a region of the Lublin Upland, in eastern Poland (Fig. 1).

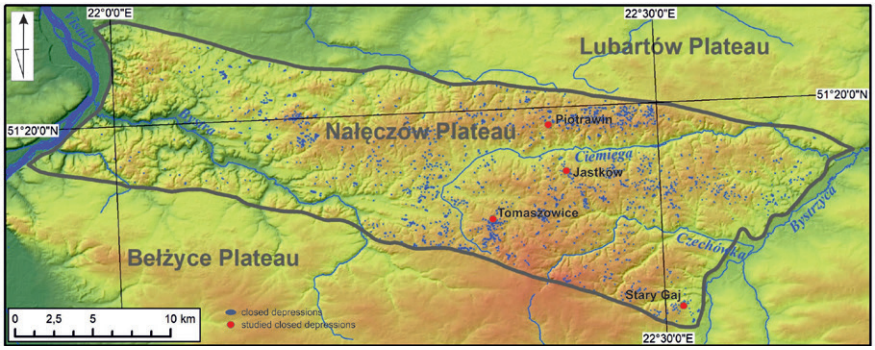

Fig. 1. Location of the study area

The bedrock of the study area is composed of Upper Cretaceous opokas and marls covered by glacigenic sediments (glacial tills, sands with gravels and clays) accumulated during the Elsterian and Odranian Glaciation (Harasimiuk 1987). Glacigenic sediments underlie the loess cover whose thickness ranges from several meters to more than 20 m (Harasimiuk and Henkiel 1976). The loess cover was formed mainly during the last glaciation, and loess accumulation lasted until 15,000–12,000 BP (Maruszczak 1976, 1980).

The undulating loess plateau, rising up to 210–250 m a.s.l., is the main landform in the study area. Numerous oval-shaped closed depressions occur on the plateau top (Fig. 1). Most of them have a diameter ranging from 25 m to 50 m (Kołodyńska-Gawrysiak and Chabudziński 2012). The loess plateau is dissected by erosion-denudation valleys forming multi-branched systems. Detailed investigations were conducted within 4 CDs (Table 1).

Table 1. Morphometric features of the studied closed depressions

No.	Site	Current land use	Catchment area (m^2)	Mean slope gradient (°)	Diameter (m)	Maximum depth (m)
1	Jastków	cropland	1,500	2.0	40	0.7
2	Stary Gaj	forest	7,568	3.41	140	4.9
3	Piotrawin	cropland	5,116	3.8	100	2.5
4	Tomaszowice	forest	5,513	3.87	98	3.46

The morphometric features of these forms indicate that they belong to the most common group of such forms occurring in the loess areas of eastern Poland (Kołodyńska-Gawrysiak and Chabudziński 2012). Two profiles in each CD were selected for detailed investigation: in the centre and on the slope of the CD. The loess under the bottoms of the CDs is decalcified, while the slopes are built of carbonate loess with about 10% of $CaCO_3$. In the upper parts of the slopes, the depth of the decalcified loess reaches only 1.2.–2 m, and its boundary is inclined at the angle of approx. 45°.

3. METHODS

The studies were conducted in four CDs. In each CD, two profiles were located: in the bottom and on the slopes. Particle size distribution was analysed using the Malvern Mastersizer 200 analyser with the HydroG dispersion unit for 210 samples from 8 profiles in 4 CDs. Samples were collected directly from the wall of the exposure or from augerings. Bulk samples of soils and sediments were collected for analysis from each morphologically distinct horizon. The samples were prepared according to the procedure proposed by Antoine *et al*. (2013). The upper limits of fractions were established based on Soil Taxonomy (1975). Thus, the upper limit is 0.002 mm for the clay fraction, 0.05 mm for silt, and 2.0 mm for sand.

SEM analyses were conducted for 39 samples from 8 profiles in 4 CDs. The samples were taken from fossil soils and loess *in situ* on the slope and in the bottom of each CD. The samples were collected from representative horizons using metal Kubiena tins (8 cm × 6 cm × 6 cm) that preserve the structure of the soils and sediments intact. Cylindrical augers made up PCV were used to collect samples from some profiles. The augers were pressed into the soil using the percussion technique. The samples were secured against humidity loss and shock during transport to the laboratory. Sections from 10 to 15 cm long were collected for microstructural analysis by means of cutting them out directly from the loess profiles inside one-metre-long sampling augers. Microscope studies were carried out with a scanning electron microscope (SEM), JEOL model JSM 6380 LA. Undisturbed samples from the studied loess profile were cut into approx. 1 cm^3 cubes and dried using a low-temperature freeze-drying method (Tovey and Wong 1973, Smart and Tovey 1982). The qualitative description of the collected material was based on images magnified between 100 and 6,500 times. The main type of microstructure, the character of contacts between structural elements, and pore space classification were named according to the nomenclature suggested by Sergeyev *et al*. (1980), Grabowska-Olszewska *et al*. (1984), supplemented by Trzciński (2008).

The quantitative analysis of the loess was carried out using STIMAN (STructure IMage ANalysis) software. The analysis was done for 1–1.5 cm^2 samples in a broad range of magnification levels. For each samples, representative fragments of the surface were selected for analysis. Then suitable magnification levels were chosen, and images were recorded for them. The magnifications covered both the smallest and the largest structural elements so that all of them could be included in the analysis. Magnification levels from 50 to 6,400 times were used. Based on photographic documentation (a series of eight images for each sample fragment), a qualitative and quantitative analysis of the following characteristics and parameters was carried out: (1) types of microstructures and arrangement of grains and particles; (2) size, shape and character of the surface

of structural elements; (3) degree of aggregation and packing of material; (4) types of contacts and structural bonds; (5) arrangement and orientation of structural elements; (6) anisotropy of microstructure; (7) porosity; (8) basic quantitative parameters such as diameter, area, perimeter of pores; (9) content of pores of different sizes (macro-, meso-, micro- and ultrapores; partition according to Osipov *et al*. 2004); (10) content of pores of different shapes (isotropic, anisotropic, and fissure-like). The quantitative analysis was conducted pursuant to the STIMAN software manual (Sokolov *et al*. 2002, Trzciński 2004).

4. RESULTS

4.1. Selected characteristics of loess grain-size distribution

4.1.1. Loess forming the bottoms of the CDs

The silt fraction predominates in the loess profiles under study, its content usually reaching 90–93%, sporadically decreasing to 88–89%. The sand fraction content usually does not exceed 2%, increasing to 3–5% in a few samples (Table 2). The clay fraction content varies considerably depending on the depth of the analysed profiles (Fig. 2). In the Jastków profile, the clay fraction content ranges from approx. 7 to approx. 11%. Initially, it increases gradually to the depth of 1.6 m where it reaches 10.82%, and then it falls to about 7% at the depth of 2.4 m. From there, the clay fraction content fluctuates, showing a generally increasing trend, reaching about 10% at the depth of 5.6 m. The mean grain diameter (Mz) ranges from 0.012 to 0.027 mm (Table 2, Fig. 2).

In the Piotrawin profile, the clay fraction content ranges from approx. 5 to approx. 10% at the depth of 1.7 m. In the deeper parts of the profile (deeper than 2 m), the clay fraction content ranges from approx. 6 to approx. 8%, and at the depth of 3.5 m it begins to decrease to reach the level of 5.12%. The mean grain diameter in the profile ranges from 0.015 to 0.03 mm (Table 2, Fig. 2).

In the Tomaszowice profile, the clay fraction content ranges from about 4.4% to about 6.6% down to the depth of 2 m. From the depth of 2 m to 5 m, it becomes stable at the level of 6–7% or more. The mean grain diameter reaches the highest level (0.03 mm) at the depth of 0.6 to 1.6 m. In the deeper part of the profile, it falls to 0.19–0.023 mm. (Table 2, Fig. 2). In the Stary Gaj profile, the clay fraction content ranges from about 4.8% to about 8.27% down to the depth of about 2 m. Its variation is smaller in the deeper part of the profile than in upper part: it varies from 5.5 to 8%. The mean grain diameter in the profile ranges from 0.017 to 0.026 mm (Table 2, Fig. 2).

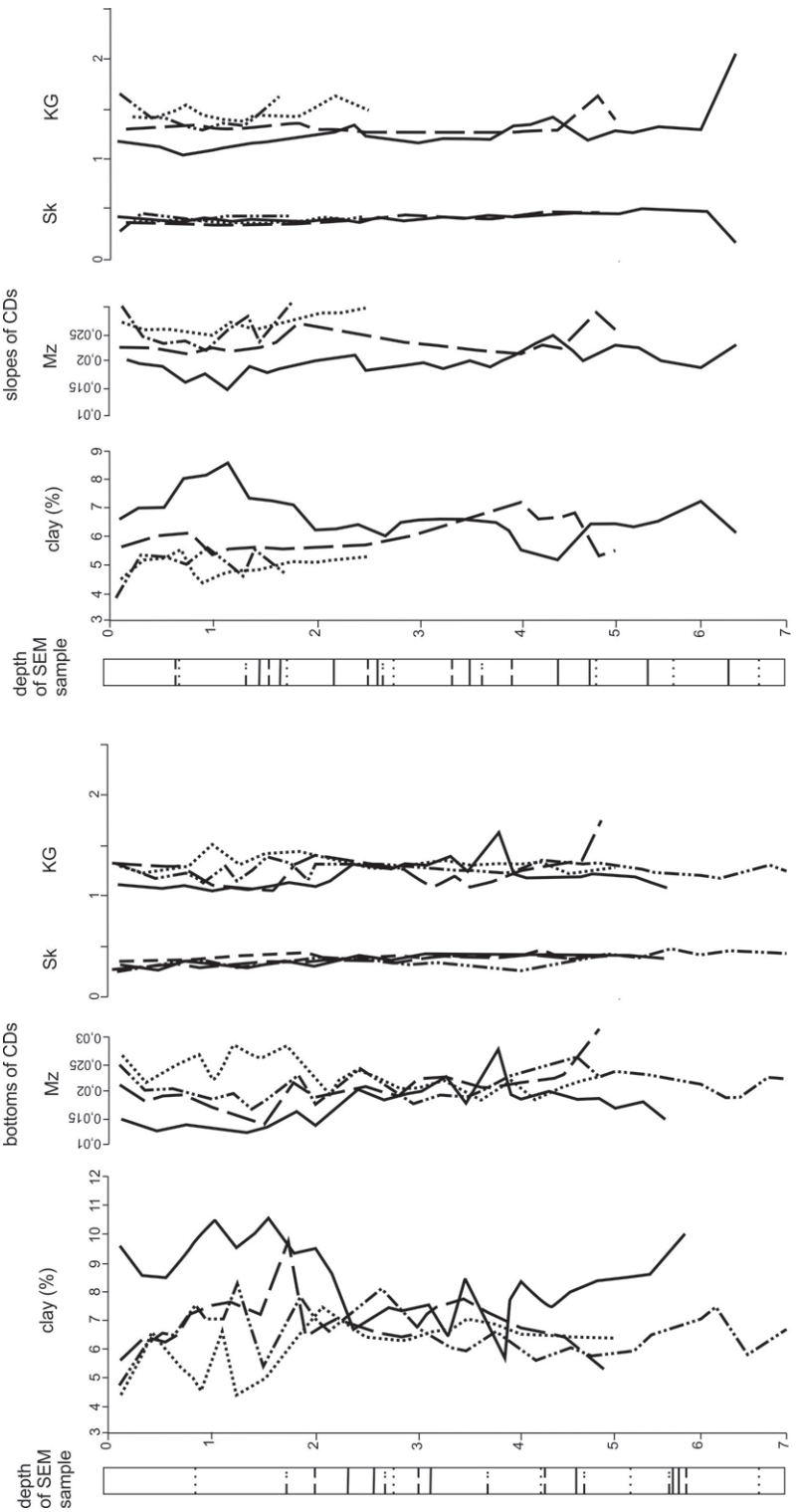

Fig. 2. Selected grain-size distribution characteristics of the loess forming the bottoms and slopes of the CDs
Mz – mean grain diameter index, Sk – skewness index, KG – kurtosis index

Table 2. Grain-size distribution of the loess forming the bottoms and slopes of the CDs

Jastków							Stary Gaj							Piotrawin							Tomaszowice						
bottoms of CDs																											
Depth m	%			Mz	SkI	KG	Depth m	%			Mz	SkI	KG	Depth m	%			Mz	SkI	KG	Depth m	%			Mz	SkI	KG
	>0.002 mm	0.002–0.05 mm	0.05–2.0 mm					>0.002 mm	0.002–0.05 mm	0.05–2.0 mm					>0.002 mm	0.002–0.05 mm	0.05–2.0 mm					>0.002 mm	0.002–0.05 mm	0.05–2.0 mm			
0.05–0.15	9.62	89.64	0.73	0.014	0.33	1.07	0.0–0.1	4.88	91.60	3.51	0.025	0.31	1.36	0.1–0.2	5.54	93.50	0.94	0.022	0.34	1.33	0–0.1	4.41	93.92	1.66	0.026	0.35	1.35
0.3–0.4	8.64	91.20	0.14	0.013	0.29	1.09	0.2–0.3	6.13	91.64	2.21	0.025	0.34	1.23	0.2–0.25	6.19	93.54	0.26	0.019	0.33	1.32	0.15–0.2	6.03	93.00	0.95	0.021	0.37	1.26
0.56–0.66	8.51	91.36	0.12	0.013	0.28	1.07	0.4–0.5	6.59	92.55	0.85	0.021	0.38	1.19	0.3–0.4	6.05	93.54	0.40	0.020	0.34	1.30	0.3–0.35	6.47	92.56	0.95	0.021	0.38	1.24
0.7–0.8	9.67	90.06	0.25	0.014	0.32	1.08	0.6–0.7	6.34	92.70	0.94	0.020	0.39	1.21	0.5–0.6	6.21	93.40	0.37	0.020	0.35	1.31	0.45–0.5	6.08	92.95	0.96	0.022	0.37	1.24
0.9–1.0	10.35	89.08	0.55	0.014	0.31	1.02	0.7–0.8	7.51	89.38	3.09	0.021	0.35	1.19	0.6–0.7	6.46	93.24	0.29	0.017	0.31	1.24	0.6–0.65	5.24	93.56	1.18	0.026	0.38	1.28
1.1–1.2	9.57	90.23	0.18	0.013	0.30	1.06	0.8–0.9	6.94	92.26	0.79	0.019	0.36	1.14	0.7–0.8	7.01	92.42	0.56	0.018	0.34	1.18	0.7–0.75	4.97	94.01	1.00	0.027	0.40	1.46
1.24–1.34	10.05	89.76	0.18	0.012	0.29	1.03	1.0–1.1	6.96	91.12	1.91	0.018	0.38	1.28	0.9–1.0	7.48	91.76	0.75	0.018	0.36	1.15	0.85–0.9	4.70	93.66	1.62	0.029	0.39	1.49
1.52–1.62	10.82	89.03	0.13	0.013	0.35	1.06	1.1–1.2	8.27	91.21	0.51	0.020	0.40	1.17	1.2–1.3	7.58	91.69	0.71	0.018	0.37	1.14	1.0–1.05	6.63	91.78	1.57	0.024	0.40	1.51
1.65–1.75	9.08	89.30	1.61	0.016	0.35	1.15	1.2–1.3	6.98	92.44	0.57	0.017	0.38	1.25	1.4–1.5	7.07	92.05	0.87	0.019	0.37	1.17	1.2–1.25	4.22	94.22	1.55	0.029	0.43	1.38
1.9–2.0	9.46	90.15	0.38	0.014	0.33	1.12	1.4–1.5	5.20	93.75	1.04	0.019	0.38	1.38	1.6–1.7	9.84	89.63	0.51	0.015	0.35	1.13	1.4–1.5	5.00	93.51	1.48	0.026	0.36	1.45
2.05–2.15	8.59	90.65	0.75	0.016	0.35	1.13	1.7–1.8	6.43	92.71	0.85	0.024	0.36	1.29	1.8–1.9	6.10	92.70	1.18	0.023	0.38	1.34	1.5–1.6	5.17	93.51	1.31	0.027	0.38	1.42
2.3–2.4	6.80	92.26	0.93	0.021	0.39	1.30	1.8–1.9	7.95	91.48	0.56	0.020	0.37	1.21	2.0–2.1	6.84	92.48	0.67	0.020	0.39	1.36	1.8–1.9	6.60	92.35	1.04	0.022	0.39	1.48
2.6–2.7	7.47	91.88	0.64	0.018	0.37	1.24	1.9–2.0	6.92	92.25	0.81	0.017	0.36	1.26	2.2–2.3	7.01	92.31	0.66	0.019	0.38	1.29	2.1–2.2	7.14	92.07	0.77	0.019	0.40	1.33
2.77–2.87	7.15	92.23	0.60	0.019	0.38	1.28	2.1–2.2	6.60	92.74	0.64	0.019	0.34	1.26	2.4–2.6	6.53	92.57	0.88	0.020	0.37	1.28	2.4–2.5	6.41	92.48	1.09	0.022	0.38	1.27
3.0–3.1	7.65	91.30	1.03	0.020	0.41	1.26	2.5–2.6	8.03	91.58	0.38	0.019	0.33	1.21	2.6–2.7	6.47	92.40	1.11	0.021	0.40	1.25	2.7–2.8	6.22	92.38	1.39	0.023	0.40	1.33
3.2–3.34	6.12	92.94	0.92	0.023	0.41	1.39	2.9–3.0	6.68	92.32	0.98	0.016	0.37	1.25	2.8–2.9	6.47	92.08	1.44	0.022	0.42	1.26	3.0–3.1	6.70	92.18	1.11	0.022	0.39	1.32
3.35–3.45	8.52	90.98	0.48	0.017	0.40	1.20	3.3–3.4	6.00	92.97	1.02	0.020	0.39	1.25	3.0–3.1	7.05	91.61	1.32	0.020	0.41	1.15	3.3–3.4	6.53	92.29	1.16	0.022	0.41	1.35
3.7–3.8	5.70	92.51	1.77	0.027	0.40	1.53	3.5–3.6	5.96	92.71	1.31	0.022	0.42	1.28	3.2–3.3	7.32	91.62	1.04	0.020	0.41	1.17	3.5–3.6	7.07	92.92	0	0.019	0.39	1.31
3.82–3.92	7.96	90.85	1.18	0.019	0.41	1.22	3.7–3.8	6.53	92.32	1.14	0.023	0.40	1.23	3.4–3.5	7.83	91.40	0.76	0.018	0.39	1.13	4.0–4.1	6.53	92.15	1.31	0.021	0.45	1.30

Jastków							Stary Gaj						Piotrawin						Tomaszowice					
bottoms of CDs																								
Depth m	%			Mz	SkI	KG	Depth m	%			Mz	SkI	KG	Depth m	%			Mz	SkI	KG	Depth m	%			Mz	SkI	KG
	>0.002 mm	0.002–0.05 mm	0.05–2.0 mm					>0.002 mm	0.002–0.05 mm	0.05–2.0 mm					>0.002 mm	0.002–0.05 mm	0.05–2.0 mm					>0.002 mm	0.002–0.05 mm	0.05–2.0 mm			
3.92–4.02	8.13	91.05	0.81	0.018	0.40	1.20	4.1–4.2	5.50	92.66	1.83	0.021	0.45	1.38	3.6–3.7	7.28	91.63	1.08	0.020	0.42	1.14	4.4–4.5	6.48	92.30	1.20	0.022	0.37	1.26
4.25–4.35	7.48	91.43	1.08	0.019	0.40	1.21	4.5–4.6	5.94	92.61	1.43	0.026	0.42	1.30	3.9–4.0	6.84	91.72	1.42	0.021	0.42	1.22	4.9–5.0	6.27	92.61	1.11	0.022	0.39	1.30
4.52–4.62	7.98	91.46	0.55	0.018	0.41	1.21	4.7–4.8	5.88	93.05	1.05	0.023	0.44	1.36	4.3–4.4	6.75	91.47	1.76	0.022	0.40	1.27	–	–	–	–	–	–	–
4.7–4.8	8.31	91.15	0.53	0.018	0.43	1.23	4.9–5.0	5.87	92.91	1.21	0.023	0.43	1.36	4.5–4.6	6.43	92.11	1.45	0.023	0.42	1.33	–	–	–	–	–	–	–
4.92–5.2	8.52	91.22	0.25	0.017	0.42	1.20	5.1–5.2	5.93	93.10	0.95	0.024	0.42	1.33	4.7–4.8	5.12	91.58	3.29	0.031	0.45	1.57	–	–	–	–	–	–	–
5.2–5.3	8.60	90.48	0.90	0.018	0.42	1.14	5.3–5.4	6.46	92.73	0.80	0.023	0.41	1.24	–	–	–	–	–	–	–	–	–	–	–	–	–	–
5.54–5.64	9.85	89.67	0.47	0.015	0.39	1.06	5.9–6.0	7.02	91.99	0.97	0.021	0.38	1.20	–	–	–	–	–	–	–	–	–	–	–	–	–	–
–	–	–	–	–	–	–	6.1–6.2	7.31	91.75	0.92	0.019	0.40	1.21	–	–	–	–	–	–	–	–	–	–	–	–	–	–
–	–	–	–	–	–	–	6.5–6.6	5.88	93.08	1.02	0.019	0.41	1.29	–	–	–	–	–	–	–	–	–	–	–	–	–	–
–	–	–	–	–	–	–	6.7–6.8	6.35	87.93	5.70	0.022	0.33	1.34	–	–	–	–	–	–	–	–	–	–	–	–	–	–
–	–	–	–	–	–	–	6.9–7.0	6.68	92.31	0.99	0.022	0.41	1.25	–	–	–	–	–	–	–	–	–	–	–	–	–	–
slopes of CDs																								
0.05–0.15	6.60	92.33	1.06	0.020	0.38	1.19	0.0–0.1	3.95	89.62	6.41	0.031	0.25	1.53	0.0–0.1	5.66	93.22	1.11	0.022	0.36	1.32	0.05–0.1	4.24	94.60	1.14	0.028	0.34	1.43
0.2–0.3	6.92	92.27	0.79	0.019	0.37	1.16	0.2–0.3	5.17	93.87	0.94	0.024	0.37	1.43	0.1–0.2	5.99	92.90	1.10	0.022	0.36	1.32	0.2–0.25	4.94	93.81	1.24	0.026	0.37	1.39
0.57–0.67	6.96	92.33	0.69	0.018	0.35	1.14	0.4–0.4	5.16	94.09	0.74	0.023	0.34	1.40	0.5–0.6	6.12	93.09	0.77	0.021	0.34	1.37	0.35–0.4	5.17	93.51	1.30	0.025	0.39	1.41
0.7–0.8	7.96	91.79	0.24	0.015	0.33	1.08	0.6–0.7	4.96	94.01	1.01	0.024	0.34	1.34	0.7–0.8	5.45	93.74	0.79	0.022	0.32	1.37	0.53–0.6	5.66	93.56	0.77	0.025	0.38	1.52
0.9–1.0	8.08	91.36	0.55	0.017	0.36	1.14	0.8–0.9	5.60	93.37	1.02	0.022	0.34	1.31	0.9–1.0	5.27	93.97	0.75	0.023	0.33	1.36	0.75–0.78	4.86	94.02	1.10	0.026	0.36	1.42
1.1–1.2	8.48	91.21	0.29	0.015	0.34	1.14	1.0–1.1	4.96	93.76	1.26	0.025	0.38	1.37	1.1–1.2	5.54	93.62	0.82	0.022	0.34	1.32	0.9–0.95	4.45	94.23	1.31	0.027	0.36	1.43
1.3–1.4	7.27	92.03	0.68	0.018	0.35	1.19	1.2–1.3	4.74	93.48	1.77	0.028	0.39	1.43	1.3–1.4	5.61	93.08	1.29	0.023	0.36	1.30	1.05–1.1	4.88	93.53	1.58	0.025	0.34	1.36
1.45–1.55	7.17	92.34	0.48	0.017	0.33	1.21	1.35–1.4	5.88	92.92	1.18	0.024	0.38	1.45	1.5–1.6	5.54	92.79	1.65	0.024	0.38	1.32	1.2–1.3	4.92	93.52	1.55	0.026	0.36	1.38

Jastków							Stary Gaj							Piotrawin							Tomaszowice						
bottoms of CDs																											
Depth m	%			Mz	SkI	KG	Depth m	%			Mz	SkI	KG	Depth m	%			Mz	SkI	KG	Depth m	%			Mz	SkI	KG
	>0.002 mm	0.002–0.05 mm	0.05–2.0 mm					>0.002 mm	0.002–0.05 mm	0.05–2.0 mm					>0.002 mm	0.002–0.05 mm	0.05–2.0 mm					>0.002 mm	0.002–0.05 mm	0.05–2.0 mm			
1.65–1.75	6.95	92.36	0.68	0.018	0.34	1.24	1.5–1.6	4.60	93.89	1.49	0.031	0.38	1.63	1.7–1.8	5.30	92.50	2.19	0.027	0.43	1.44	1.5–1.6	4.62	93.74	1.63	0.027	0.35	1.43
1.83–1.93	6.10	93.11	0.78	0.020	0.34	1.26	–	–	–	–	–	–	–	3.9–4.0	7.14	91.47	1.38	0.021	0.43	1.27	1.7–1.8	5.09	92.81	2.08	0.028	0.40	1.46
1.93–2.03	6.14	93.21	0.64	0.020	0.36	1.28	–	–	–	–	–	–	–	4.1–4.2	6.64	91.41	1.93	0.023	0.42	1.27	2.1–2.2	5.07	93.79	1.12	0.028	0.38	1.56
2.1–2.2	6.28	92.76	0.94	0.020	0.34	1.22	–	–	–	–	–	–	–	4.3–4.4	6.73	91.69	1.56	0.022	0.40	1.27	2.4–2.5	5.18	92.74	2.06	0.029	0.40	1.51
2.3–2.4	5.80	93.36	0.83	0.021	0.37	1.28	–	–	–	–	–	–	–	4.5–4.6	6.91	91.13	1.94	0.023	0.46	1.29	–	–	–	–	–	–	–
2.45–2.5	6.49	93.01	0.49	0.018	0.35	1.20	–	–	–	–	–	–	–	4.7–4.8	5.39	92.19	2.40	0.028	0.47	1.52	–	–	–	–	–	–	–
2.62–2.72	6.65	92.78	0.55	0.019	0.36	1.24	–	–	–	–	–	–	–	4.9–5.0	5.58	92.37	2.03	0.026	0.45	1.40	–	–	–	–	–	–	–
2.97–3.07	6.50	92.63	0.85	0.020	0.38	1.2	–	–	–	–	–	–	–	–	–	–	–	–	–	–	–	–	–	–	–	–	–
3.15–3.25	6.64	92.99	0.35	0.018	0.36	1.23	–	–	–	–	–	–	–	–	–	–	–	–	–	–	–	–	–	–	–	–	–
3.35–3.45	6.53	92.62	0.84	0.020	0.39	1.25	–	–	–	–	–	–	–	–	–	–	–	–	–	–	–	–	–	–	–	–	–
3.6–3.7	6.48	92.96	0.54	0.019	0.37	1.23	–	–	–	–	–	–	–	–	–	–	–	–	–	–	–	–	–	–	–	–	–
3.8–3.9	6.23	93.03	0.73	0.021	0.38	1.27	–	–	–	–	–	–	–	–	–	–	–	–	–	–	–	–	–	–	–	–	–
4.0–4.1	5.71	93.42	0.85	0.023	0.40	1.39	–	–	–	–	–	–	–	–	–	–	–	–	–	–	–	–	–	–	–	–	–
4.26–4.36	5.48	93.45	1.06	0.025	0.41	1.44	–	–	–	–	–	–	–	–	–	–	–	–	–	–	–	–	–	–	–	–	–
4.4–4.5	5.98	93.20	0.81	0.022	0.42	1.34	–	–	–	–	–	–	–	–	–	–	–	–	–	–	–	–	–	–	–	–	–
4.57–4.67	6.73	92.58	0.67	0.020	0.41	1.22	–	–	–	–	–	–	–	–	–	–	–	–	–	–	–	–	–	–	–	–	–
4.96–5.06	6.73	92.19	1.07	0.022	0.45	1.30	–	–	–	–	–	–	–	–	–	–	–	–	–	–	–	–	–	–	–	–	–
5.06–5.16	6.58	92.40	1.00	0.022	0.43	1.34	–	–	–	–	–	–	–	–	–	–	–	–	–	–	–	–	–	–	–	–	–
5.5–5.6	6.87	92.50	0.62	0.020	0.43	1.26	–	–	–	–	–	–	–	–	–	–	–	–	–	–	–	–	–	–	–	–	–
5.9–6.0	7.12	92.61	0.25	0.019	0.43	1.26	–	–	–	–	–	–	–	–	–	–	–	–	–	–	–	–	–	–	–	–	–
6.4–6.5	6.17	88.23	5.59	0.023	0.15	2.07	–	–	–	–	–	–	–	–	–	–	–	–	–	–	–	–	–	–	–	–	–

4.1.2. Loess forming the slopes of CDs

The silt fraction predominates in the loess profiles under study, its content usually reaching 90–94%. The sand fraction content is usually 1–2%, reaching 5–6% in a few samples (Table 2, Fig. 2).

In the Jastków profile, the sand fraction content ranges from approx. 5.5 to approx. 8.5%. Initially, it increases to reach its maximum level of 8.5% at the depth of 1.2 m, then it falls to about 6% at the depth of 4.5 m, and then increases to about 7% in the deepest part of the profile. The mean grain diameter shows small variation: from about 0.015 to about 0.025 mm (Table 2, Fig. 2). In the Piotrawin profile, the clay fraction content is at the level of about 5–6%, and then increases to about 7% at the depth of 4.0–4.6 m. In the deepest part of the profile, it falls to about 5.5%. The mean grain diameter ranges from 0.021 to 0.028 mm (Table 2, Fig. 2). In the Tomaszowice profile, the clay fraction content increases to 5.6% down to the depth of 0.6 m, and then it remains at a similar level of about 4.5–5% down to the depth of 2.5 m. The main grain diameter shows small variation with depth: from about 0.025 to 0.029 mm at the depth of 2.5 m. (Table 2, Fig. 2). In the Stary Gaj profile, the clay fraction content increases to approx. 5.6% at the depth of 0.9 m. It fluctuates at the level of 5–6% with increasing depth. The mean grain diameter ranges from 0.03 to 0.022 mm (Table 2, Fig. 2).

Sk and KG indices (skewness and kurtosis of grain-size distribution respectively) have similar values in the loess forming the bottoms and the slopes of the depressions, but in the bottoms they show greater variation with increasing depth than on the slopes (Table 2, Fig. 2).

4.2. Loess microstructure

4.2.1. Loess forming the bottoms of CDs

Qualitative description

Loess in the bottoms of the CDs mostly have a matrix microstructure except for the J2_4, SG15_1, TK1_4 horizon where they have a skeletal microstructure (Fig. 3). Matrix microstructure consists of clay matter, referred to as the matrix, with irregularly distributed isolated clay particles. The clay matrix is formed by clay microaggregates and aggregates. In the Jastków profile (J2) and Tomaszowice profile (TK1), the degree of packing of this microstructure changes with the increasing depth of the profile from loosely packed (J2_1, TK1_1) to medium packed (J2_2, J2_3, J2_5, TK1_2, TK1_3, TK1_5). In the Stary Gaj profile, the degree of packing of this microstructure does not change in the vertical profile; its structural elements show are densely packed (Fig. 3). In the Piotrawin pro-

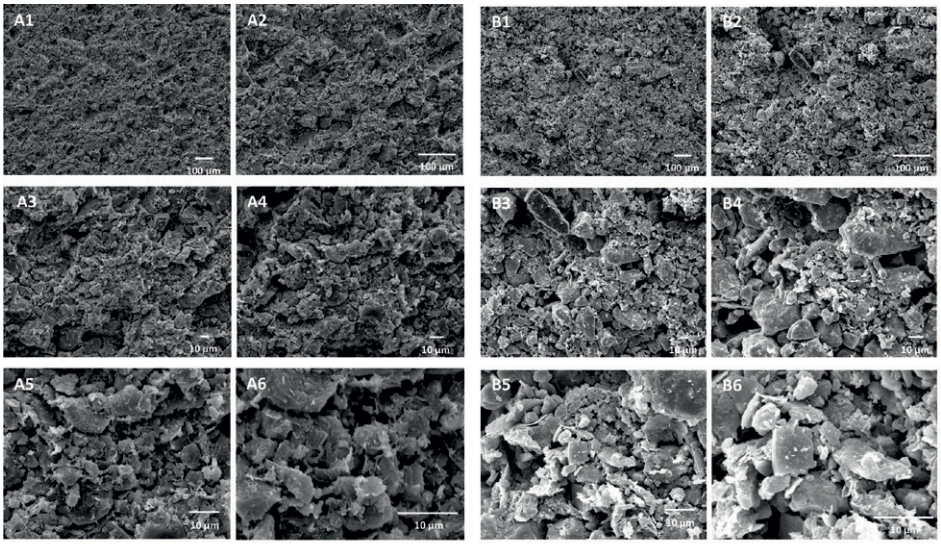

Enlargement: A1, B1 – 100x, A2, B2 – 200x, A3, B3 – 400x, A4, B4 – 800x, A5, B5 – 1600x, A6, B6 – 3300x. A – the bottom of CD, Stary Gaj profile SG15_4, the matrix microstructure with high degree of packing (A1, A2), the contacts are of the facies–edge type (F–E) – A5, rarely of the surface–surface type (F–F) – A6, the number of contacts of the F–F type and the orientation of structural elements increase with depth, the microstructure more oriented (anisometric – A3, A4). Micropores were transformed from isometric micropores to anisometric micropores (A4, A6). The large micropores were reduced and the smallest micropores, up to 1–2 μm in diameter, are the most numerous (A6). Larger micropores became "closed" or partially closed, and the matrix microstructure became densely packed. B – the slope of CD, Jastków profile J3_8, the moderately packed skeleton microstructure (B1, B2), clay matter is unevenly distributed in irregular concentrations (B3, B4), the contacts are of the facies–edge type (F–E) – B5 rarely of the surface–surface type (F–F) – B6, and only sometimes of the edge–edge (E–E) type – B6, the lack or a very weak orientation of structural elements and low degree of microstructure anisotropy (B4). Pore space consists of larger, isometric interaggregate pores and smaller, isometric inter- and intra-aggregate pores (B5, B6). Loosely packed clay microaggregates combined to form aggregates with a greater degree of packing. Most of the large micropores became partially "closed", pores of smaller dimensions became totally "closed".

Fig. 3. Microstructure of the loess forming the CDs

file, the degree of packing ranges from medium (P_1) to high (P1_2-P1_4). The contacts between clay microaggregates in the matrix microstructure are usually of the face to edge type (F–E), more rarely of the face to face type (F–F) – J2_5 (Fig. 3). The number of contacts of the F–F type increases with depth. In the Jastków and Tomaszowice profiles, a weak orientation of clay microaggregates can be observed (J2_3 and J2_4). In the Stary Gaj and Piotrawin profiles, the orientation of structural elements increases with depth and, consequently, the microstructure becomes more oriented, i.e. anisometric (Fig. 3). Micropores in the loess profiles under study were transformed from isometric micropores in the upper part of the profiles to anisometric in the deeper parts (profile J2, SG, P1). Changes occurred in the pore space of the profiles under study. Most of the large micropores were transformed, and their dimensions were reduced so that the smallest micropores, up to 1–2 μm in diameter, are the most numerous (Fig. 3). Larger micropores became "closed", or partially closed (Tomaszowice TK1_5 profile), and the matrix microstructure became densely packed (Fig. 3). In the Jastków profile, (J2) the microstructure also features a few large micropores and smaller mesopores.

Table 3. Selected quantitative parameters of the microstructure of the loess forming the bottoms of CDs

Parameters	Jastków					Piotrawin						Stary Gaj					Tomaszowice				
Sample name Depth [cm]	J2_1 220	J2_2 260	J2_3 307	J2_4 460	J2_5 570	SG15_1 180	SG15_2 270	SG15_3 370	SG15_4 470	SG15_5 570	SG15_6 580	P1_1 200	P1_2 300	P1_3 420	P1_4 590	TK1_1 90	TK1_2 280	TK1_3 420	TK1_4 510	TK1_5 680
Number of pores N x 10^3	400,163	537,074	702,084	630,268	556,209	578,008	602,481	295,335	479,130	543,480	535,470	422,344	447,112	393,368	429,770	714,546	520,108	526,030	356,723	472,229
Porosity n [%]	42.79	37.35	38.47	45.71	39.33	34.39	40.74	35.87	34.78	35.47	34.18	36.68	37.19	35.49	34.83	33.26	35.92	36.62	38.76	29.99
Total pores area St [µm^2] x 10^3	498,710	435,009	452,122	540,367	457,581	391,597	477,995	414,300	402,281	413,597	394,852	426,877	430,860	416,172	403,787	384,144	413,830	428,171	457,505	348,150
Maximum pores area S_{max} [µm^2]	9821.00	5834.00	8129.00	10566.00	7277.00	4830.00	4600.00	12909.00	4452.00	6683.00	6177.00	3607.00	13143.00	8639.00	4346.00	10471.00	5702.00	8662.00	8078.00	3237.00
Minimum pores area S_{min} [µm^2]	0.01	0.01	0.01	0.01	0.01	0.01	0.01	0.01	0.01	0.01	0.01	0.01	0.01	0.01	0.01	0.01	0.01	0.01	0.01	0.01
Average pores area S_{av} [µm^2]	1.25	0.81	0.64	0.86	0.82	0.68	0.79	1.40	0.84	0.76	0.74	1.01	0.96	1.06	0.94	0.54	0.80	0.81	1.28	0.74
Total pores perimeter Pt [µm] x 10^3	1,259,937	1,274,561	1,559,372	1,418,891	1,406,079	1,544,358	1,503,604	1,108,479	1,338,705	1,317,293	1,343,385	1,180,092	1,287,857	1,123,561	1,201,783	1,445,099	1,430,938	1,225,531	966,097	1,179,140
Maximum pores perimeter P_{max} [µm]	5102.00	3067.00	3756.00	4762.00	3792.00	4028.00	3068.00	7106.00	1968.00	3082.00	2448.00	1684.00	7338.00	3502.00	2308.00	5140.00	2472.00	3858.00	3806.00	1714.00
Minimum pores perimeter P_{min} [µm]	0.44	0.50	0.47	0.56	0.47	0.53	0.41	0.56	0.50	0.47	0.50	0.47	0.44	0.53	0.53	0.38	0.50	0.50	0.50	0.53
Average pores perimeter P_{av} [µm]	3.15	2.37	2.22	2.25	2.53	2.67	2.50	3.75	2.79	2.42	2.51	2.79	2.88	2.86	2.80	2.02	2.75	2.33	2.71	2.50
Maximum pores diameter D_{max} [µm]	111.82	86.19	101.74	115.99	96.26	78.42	76.53	128.20	75.29	92.24	88.68	67.77	129.36	104.88	74.39	115.46	85.21	105.02	101.42	64.20
Minimum pores diameter D_{min} [µm]	0.08	0.08	0.08	0.08	0.08	0.08	0.08	0.08	0.08	0.08	0.08	0.08	0.08	0.08	0.08	0.08	0.08	0.08	0.08	0.08
Average pores diameter D_{av} [µm]	0.37	0.27	0.25	0.24	0.30	0.34	0.30	0.46	0.34	0.30	0.30	0.33	0.35	0.34	0.33	0.24	0.32	0.28	0.33	0.32
Ultrapores [%]	0.1	0.3	0.3	0.3	0.2	0.2	0.2	0.1	0.2	0.2	0.2	0.2	0.2	0.1	0.1	0.5	0.2	0.3	0.1	0.3
Micropores [%]	30.4	33.7	29.8	22.1	33.1	53.2	29.7	39.4	41.0	34.5	39.8	34.0	35.7	29.6	36.4	37.8	33.9	31.6	19.9	37.5
Mezopores [%]	69.5	66.0	69.9	77.6	66.7	46.6	70.1	60.5	58.8	65.3	59.9	65.8	64.1	70.3	63.5	61.7	65.9	68.1	80.0	62.3
Average form index of pores K_{fav} [-]	0.494	0.518	0.510	0.496	0.513	0.504	0.497	0.502	0.515	0.507	0.507	0.550	0.492	0.504	0.511	0.480	0.513	0.499	0.481	0.498
Isometric pores [%]	16.9	20.1	18.5	20.5	24.4	17.4	19.2	20.1	23.1	22.7	24.8	31.4	15.6	19.0	21.7	13.2	25.3	19.4	17.9	21.6
Anisometric pores [%]	83.0	79.8	81.5	79.4	75.4	82.6	80.1	79.8	76.8	77.3	74.5	68.5	84.3	80.7	78.2	86.6	74.6	80.2	82.1	78.3
Fissure-like pores [%]	0.1	0.1	0.0	0.1	0.2	0.0	0.7	0.1	0.1	0.0	0.7	0.1	0.1	0.3	0.1	0.2	0.1	0.4	0.0	0.1
Microstructure anisotropy index K_a [%]	7.71	6.18	5.81	8.02	3.11	3.83	6.04	18.42	15.01	15.01	8.21	9.65	7.87	12.68	5.91	5.78	3.98	6.44	11.45	12.82
Dominant direction of pores α [°]	154	129	143	147	138	147	109	140	43	126	117	146	137	115	97	163	157	19	171	158
Specific surface area of pores [1/µm]	1.11	1.12	1.35	1.22	1.23	1.39	1.31	0.98	1.18	1.15	1.19	1.03	1.13	0.97	1.06	1.03	1.27	1.27	1.07	0.83

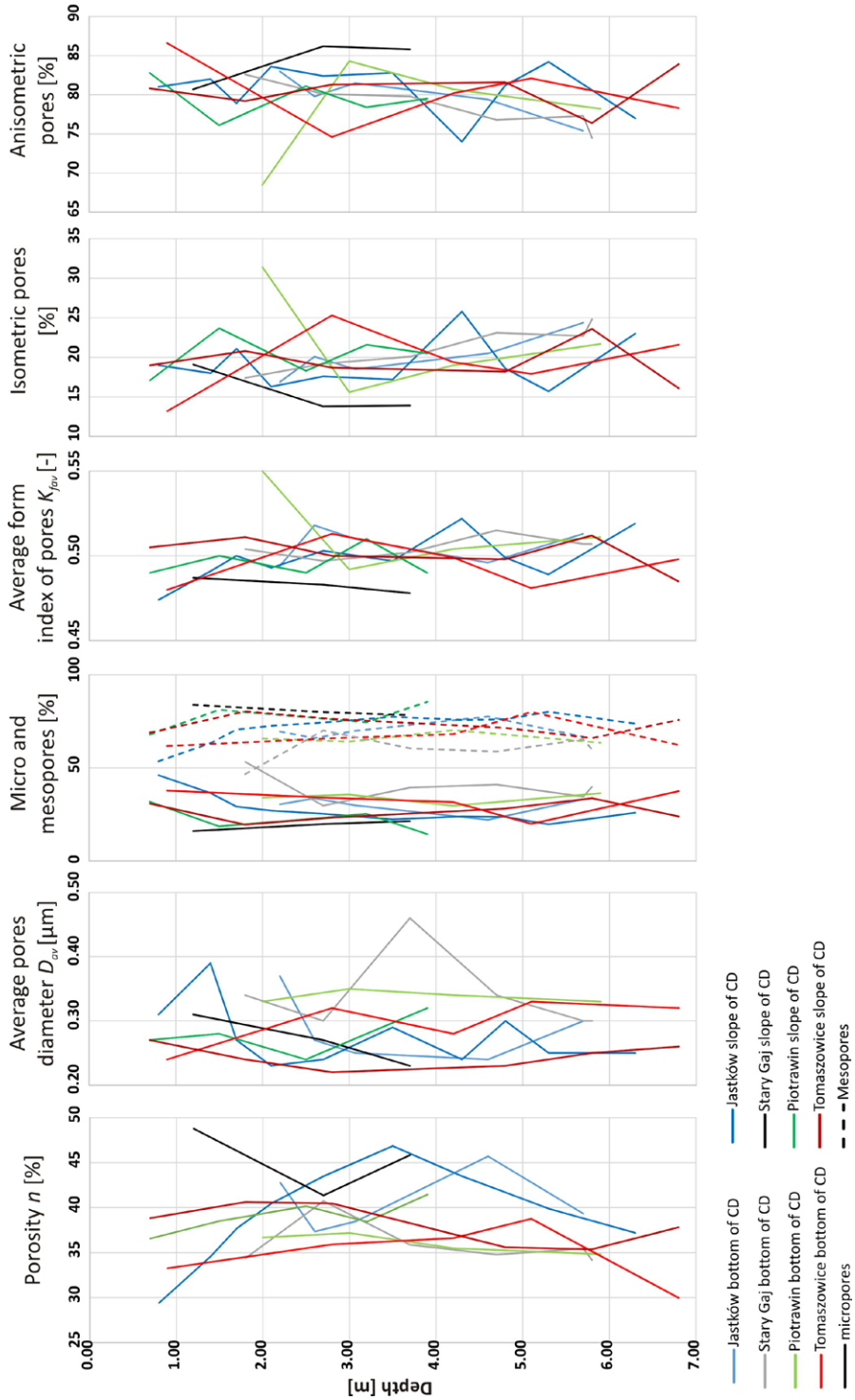

Fig. 4. Selected quantitative parameters of the microstructure of the loess forming the bottoms and the slopes of CDs

Number of pores

The number of pores (*N*) in the Jastków profile varies considerably. It increases in the upper part of the profile, but in the middle part this trend is reversed and the number of pores decreases with depth (Table 3). In the Stary Gaj profile, the number of pores increases down to the depth of 2.7–2.8 m, then it decreases by half, and then it increases again and remains stable at approx. 540,000 pores (Table 3). In the entire Piotrawin profile, the number of pores is similar: about 400,000 (Table 3). The number of pores varies considerably in the Tomaszowice profile. The largest number occurs in the shallowest part, and the smallest number in the middle part of the profile (Table 3).

Porosity

In the Jastków profile, porosity (*n*) varies from 37.3% to 45.7% (Table 3). In the Piotrawin profile, porosity varies from 34.8% to 37.1%, reaching the lowest value in the deepest part of the profile (Table 3). In the Tomaszowice profile, porosity increases with depth from 33.2% to 38.7%, and then falls to 29.9% in the deepest part of the profile (6.8–6.9 m) (Table 3). In the Stary Gaj profile, porosity ranges from 34.2% to 40.7%, reaching the lowest value in the deepest part of the profile (Table 3).

Area of the pores

The total pores area (S_t) in the Jastków profile is similar and ranges from 435,009 μm^2 at the depth of 260 cm to 540,367 μm^2 at the depth of 460 cm (Table 3). Across the entire Piotrawin profile, the total pores area is slightly above 400,000 μm^2. In the Stary Gaj profile, the value of this parameter is similar, and ranges from about 395,000 to 415,000 μm^2 except for the depth of 2.7–2.8 m where it reaches the value of 477.995 μm^2 (Table 3). In the Tomaszowice profile, the total area of the pores shows an identical growing trend as in the case of porosity, with slightly lower values at the depth of 5.3–5.4 m (Table 3). In the Tomaszowice profile, this parameter shows a growing trend down to the depth of 4.2–4.3 m, but then its value decreases with depth down to 348,150 μm^2 (Table 3).

The maximum pores area (S_{max}) in the Jastków profile changes from 5,834 μm^2 to 10,566 μm^2, and no trend can be discerned in how the values of this parameter change (Table 3). In the Piotrawin profile, the parameter initially grows to 13,143 μm^2, but then decreases to 4,346 μm^2. Similarly to the Jastków profile, no clear trend can be discerned in how the values of this parameter change in the Piotrawin profile. Extreme values were recorded in the middle part of the profile (Table 3). The maximum pores area in the Tomaszowice profile

ranges from 3,465 μm^2 at the depth of 1.7–1.8 m to 41,788 μm^2 at the depth of 6.9–7.0. Initially, down to the depth of 4.1–4.2 m, this parameter shows a clear growing trend (Table 3). In most profiles, the highest values of the maximum area of the pores occur at the depth of 3–4 m. The values of the minimum area of the pores (S_{min}) are 0.01 μm^2 for all profiles (Table 3).

In the Jastków profile, the average pores area (S_{av}) had similar values, i.e. about 0.83 μm^2, except for the depth of 220 cm where its value is the highest, 1.25 μm^2, and the depth of 307 cm where it is 0.64 μm^2. In the shallow part of the profile, the value of this parameter decreases with depth (Table 3). The average pores area is similar across the entire Piotrawin profile, and ranges from 0.94 to 1.06 μm^2. The values of this parameter are similar in the Stary Gaj profile, ranging from 0.68 to 0.84 μm^2. The value of this parameter is higher (1.40 μm^2) only at the depth of 3.7–3.8 m. Initially, it increases with depth, but it begins to decrease from the depth of 3.7–3.8 m (Table 3). In the Tomaszowice profile, the average pores area is more varied than in other profiles, and no clear trend can be observed in how the values of these parameter change.

Perimeter of the pores

The total pores perimeter (P_t) in the Jastków profile initially increases with depth, but from the depth of 460 cm it becomes stable assuming the value of about 141,000 μm (Table 3). In the Piotrawin profile, the total perimeter shows little variation, staying within the range of 1,123,561–1,287,857 μm. In the shallowest part of the Stary Gaj profile, the value of this parameter is about 1,500,000 μm, but then it falls to 1,108,479 μm, and stays in the region of 1,338,705 μm in the remaining part of the profile (Table 3). The parameter does not vary significantly in the Tomaszowice profile, ranging from 953,690 to 1,441,619 μm (Table 3).

In the Jastków profile, the maximum pores perimeter values are varied; the maximum and the minimum values of this parameter occur in the shallowest part of the profile (Table 3). Considerable variation of this parameter is observed in the Piotrawin profile, its values ranging from 1,684.00 to 7,338.00 μm, but there is no change trend depending on depth (Table 3). In the Stary Gaj profile, the values of this parameter range from about 2,000 to more than 4,000 μm. The value of this parameter is higher (7,106.00 μm^2) only at the depth of 3.7–3.8 m (Table 3). The maximum pores perimeter shows a very strong variation in the Tomaszowice profile. The lowest value of this parameter is almost 10 times lower than the highest value: 2,282.00 μm and 2,1604.00 μm, respectively. Extreme values are observed at the extreme ends of the profile. The value of this parameter decreases with depth across the entire profile (Table 3).

The values of the minimum pores perimeter (P_{min}) are very similar in the entire Jastków profile, ranging from 0.44 to 0.56 μm (Table 3). The value of

this parameter is similar across the entire Piotrawin profile: it is about 0.45 μm in the shallowest part and 0.53 μm in the deepest part (Table 3). The minimum pores perimeter is also similar across the entire Stary Gaj profile, its values ranging from 0.41 to 0.56 μm (Table 3). In the Tomaszowice profile, the minimum pores perimeter shows slight variation. The minimum value of the parameter, 0.44 μm, occurs at the depth of 4.2–4.2 m, and the highest, 0.69 μm, at the depth of 2.9–3.0 m. Besides, the parameter's values range from 0.50 to 0.53 μm (Table 3).

The average pores perimeter (P_{av}) in the Jastków profile initially decreases with depth, but from the depth of 460 cm it begins to decrease (Table 3). In the Piotrawin profile, the values of this parameter are in the 2.79–2.88 μm range (Table 3). This parameter shows greater variation in the Stary Gaj profile than in the case of the minimum pores perimeter. The minimum value of this parameter is 2.42 μm, while the maximum is 3.75 μm. The middle part of the profile is characterised by the highest values (Table 3). The average pores perimeter the Tomaszowice profile varies from 2.28 to 2.89 μm except for the depth of 2.9–3.0 m where the value of the parameter is 4.18 μm (Table 3).

Diameter of the pores

The maximum pores diameter (D_{max}) in the Jastków and Tomaszowice profiles range from 115.9 to 86.1 μm and from 115.4 to 64.2 μm, respectively, depending on the depth (Table 3). In the Stary Gaj and Piotrawin profiles the variation ranges are 128.2–75.2 μm and 129.3–74,3 μm, respectively (Table 3). The minimum pores diameter (D_{min}) does not change in the profiles under study and has the value of 0.08 μm. The average pores diameter (D_{av}) have the following variation ranges: 0.37–0.24 μm in the Jastków profile, 0.33–0.24 μm in the Tomaszowice profile, 0.46–0.30 μm in the Stary Gaj profile, and 0.33–0.35 μm in the Piotrawin profile (Table 3).

Size of the pores

The share of ultrapores is similar in all profiles, and ranges from 0.1 to 0.3% in the Jastków profile, from 0.1 to 0.5% in the Tomaszowice profile, from 0.1 to 0.2% in the Stary Gaj profile, and from 0.1 to 0.2% in the Piotrawin profile (Table 3). The share of micropores ranges from 22.1 to 33.7% in the Jastków profile, from 19.9 to 37.8% in the Tomaszowice profile, from 29.7 to 53.1% in the Stary Gaj profile, and from 29.6 to 36.4% in the Piotrawin profile. Their share varies depending on the depth. The percentage share of mesopores is varied, and ranges from 77.6 to 66.0% in the Jastków profile, from 61.7 to 80.0% in the Tomaszowice profile, from 70.1 to 46.6% in the Stary Gaj profile, and from 63.5 to 70.3% in the Piotrawin profile (Table 3).

The pore form coefficient

The average form index of pores (K_{fav}) reaches relatively low values, ranging from 0.49 to 0.51 in the Jastków profile, from 0.48 to 0.51 in the Tomaszowice profile, from 0.49 to 0.51 in the Stary Gaj profile, and from 0.49 to 0.55 in the Piotrawin profile (Table 3).

Shape of the pores

Isometric pores account for between 16.9 and 24.4% of the pores in the Jastków profile, from 17.4 to 24.7% in the Stary Gaj profile, from 15.6 to 21.8% in the Piotrawin profile, with a growing trend with increasing depth, and from 13.2 to 25.3% in the Tomaszowice profile (Table 3). Anisometric pores have the largest share in all profiles under study: from 75.4 to 83.0% (Jastków profile), from 74.6 to 86.6% (Tomaszowice profile), from 74.5 to 82.6% (Stary Gaj profile), and from 68.5 to 84.3% (Piotrawin profile). Their share generally decreases with increasing depth (Table 3). Interstitial pores account for only 0.1–0.2% (Jastków profile), 0.1–0.4% (Tomaszowice profile), 0.1–0.7% (Stary Gaj profile), and from 0.3–0.1% (Piotrawin profile). Their share is the greatest in the deepest parts of the profiles (Table 3).

Microstructure anisotropy index

The microstructure anisotropy index (K_a) ranges from 3.1 to 8.0%, reaching the the lowest value in the deepest part of the Jastków profile (Table 3). In the Tomaszowice profile, it ranges from 3.9% to 12.8%, reaching the highest values in the deepest part (Table 3). In the Stary Gaj and Piotrawin profiles, the values of this index range from 3.8 to 18.4% and from 5.9 to 12.6%, respectively. In these two profiles, the value of the index initially goes up, but then it falls with increasing depth (Table 3).

Orientation of structural elements

In almost the entire Jastków profile, the dominant direction of pores (α) is 145°. The lowest values are observed at the depth of 260 cm and 570 cm: they are 129° and 138°, respectively (Table 3). In the Stary Gaj profile, the orientation ranges from 109 to 147°, except for the depth of 4.7–4.8 m where it is 43° (Table 3). The orientation in the Piotrawin profile has the highest value at the depth of 2.0–2.05 m and 3.0–3.1 m: it is 146 and 137°, respectively. The values of this parameter range from 90 to 166 in the Tomaszowice profile (Table 3).

Specific surface area of the pores

In the Jastków profile, the specific surface area is 1.11–1.12 1/μm in its shallowest parts (Table 3). In the deepest parts of the profile, it reaches 1.22–1.23 1/μm, and the highest value can be observed in the middle part: 1.35 1/μm. The specific surface area in the Stary Gaj profile ranges from 0.98 1/μm in the middle part of the profile to 1.39 1/μm in its shallowest part (Table 3). Across the entire Piotrawin profile, the specific surface area is similar, ranging from 0.97 to 1.03 1/μm except for the depth of 3.0–3.1 m where the value of this parameter is 1.13 1/μm. The specific surface area does not vary significantly in the Tomaszowice profile. The minimum value, 0.83 1/μm, is observed at the depth of 2.9–3.0 m, while the lowest value, 1.28 1/μm, occurs at the depth of 5.3–5.4 m (Table 3). The specific surface area in the Tomaszowice profile initially remains at the level of 1.27 1/μm, but in the middle part of the profile it ranges from 0.83 1/μm to 1.07 1/μm (Table 3).

4.2.2. Loess forming the slopes of closed depressions

Qualitative description

The microstructural composition of loess in the profiles under study changes from the matrix microstructure type in the upper parts of the profiles (J3_1 – J3_4, P5_1, TK11_1) to the skeleton microstructure type in the lower parts of the profiles (J3_5 – J3_10 P5_2 – P5_5,TK11_2 – TK11_6) (Fig. 3). In the entire Stary Gaj profile, loess is exclusively of the skeletal microstructure type.

The degree of packing of the matrix microstructure varies in the individual profiles. In the Piotrawin profile, it is loosely packed (P5_2), while in the Tomaszowice profile, it is medium packed (TK11_1) (Fig. 3). In the Jastków profile, the degree of packing alternates between loosely packed (J3_1 and J3_3, P5_2) to medium packed (J3_2 and J3_4). In all the profiles under study, the contact between clay microaggregates is mainly of the faces–edge (F–E) type, secondarily, the faces–faces (F–F) type, and only sometimes of the edge–edge (E–E) type (the Jastków and Tomaszowice profiles) (Fig. 3). Pore space consists of larger, isometric interaggregate pores and smaller, isometric inter- and intra-aggregate pores (Fig. 3). The total lack of orientation of structural elements or a very weak orientation of clay aggregates and low degree of microstructure anisotropy are evident (Stary Gaj profile).

Skeletal microstructure consists mainly of silt grains between which clay material is unevenly distributed (Fig. 3). In loess with skeletal microstructure in all profiles, the degree of its packing changes with depth: from loosely packed, where a small amount of clay matter is evenly distributed (J3_5 and J3_6, SG7_1, SG7_2, P5_2 – P5_4, TK11_2, TK11_3), to medium packed, where clay matter

is unevenly distributed in irregular concentrations (J3_7 – J3_10, SG7_3, P5_5, TK11_5 and TK11_6) (Fig. 3). In the profiles at Stary Gaj (SG7_3, depth of 3.7–3.8 m), Piotrawin (P5_5, depth of 3.9–4.0 m), and Tomaszowice (TK11_4, depth of 4.8–4.9 m), the loess horizons have skeletal microstructure with almost horizontal laminae of finer, mainly clay material and, secondarily, very fine silt material. The clay microaggregates in the skeletal microstructure have no orientation (Jastków, Stary Gaj, Tomaszowice) or it is very weak (Piotrawin). Loosely packed clay microaggregates most probably combined to form aggregates with a greater degree of packing. Changes occurred in the pore space. Most of the large micropores became partially "closed" (SG7_3, P5_5), while pores of smaller dimensions became totally "closed" (J3_1 – J3_3, Tomaszowice). There are also a few large micropores and smaller mesopores (Jastków, Tomaszowice).

Number of pores

In the Jastków profile, the number of pores (*N*) does not decrease with depth, which is the case in the Stary Gaj profile where the growing trend with increasing depth is clear (Table 4). In the Piotrawin profile, the number of pores decreases down to the depth of 1.55 m, increases by half at the depth of 2.5 m, but then the trend is reversed and the number of pores decreases again with increasing depth. In the Tomaszowice profile, the value of this parameter increases and decreases alternately (Table 4).

Porosity

Porosity (*n*) varies from 29.4% to 46.8% in the Jastków profile, from 36.5 to 41.7% in the Piotrawin profile, fluctuating and reaching the lowest value in the deepest part of the profile (Table 4). In the Tomaszowice profile, porosity increases with depth from 38.8% to 40.4%, and then falls to 37.8% in the deepest part of the profile (6.8–6.9 m). In the Stary Gaj profile, porosity ranges from 48.7% to 45.8% in the deepest part of the profile (Table 4).

Area of the pores

In the Jastków profile, the total pores area (sum of the area of all pores) (S_t) initially increases with depth, reaching the maximum value of 552,611 μm^2 at the depth of 350 cm. In the lower part of the profile, the values decreases to 435,800 μm^2 (Table 4). In the Stary Gaj profile, this parameter does not show a clear trend, ranging from 488,512 to 581,791 μm^2 (Table 4). Across the entire Piotrawin profile, the value of this parameter changes within the 428,690–495,269 μm^2 range. Despite the absence of a clear trend, this parameter reaches its lowest value in the shallowest part of the profile, and the highest value in

Table 4. Selected quantitative parameters of the microstructure of the loess forming the slopes of CDs

Parameters	Jastków										Stary Gaj			Piotrawin					Tomaszowice					
Probe no. Depth [cm]	J3_1 80	J3_2 140	J3_3 170	J3_4 210	J3_5 270	J3_6 350	J3_7 430	J3_8 480	J3_9 530	J3_10 630	SG7_1 120	SG7_2 270	SG7_3 370	P5_1 70	P5_2 150	P5_3 250	P5_4 320	P5_5 390	TK11_1 70	TK11_2 180	TK11_3 280	TK11_4 480	TK11_5 580	TK11_6 680
Number of pores N x 10^3	460,480	356,708	522,087	782,015	727,437	501,033	831,755	465,228	590,680	656,953	417,270	553,755	983,522	648,405	489,694	734,433	633,157	312,920	677,991	635,999	876,706	911,332	798,291	617,288
Porosity n [%]	29.42	34.62	37.71	40.48	43.51	46.86	43.50	41.71	39.89	37.20	48.79	41.37	45.86	36.58	38.52	40.17	38.45	41.47	38.85	40.63	40.47	35.59	35.37	37.82
Total pores area S_t [µm^2] x 10^3	338,265	400,162	438,272	475,102	512,671	552,611	514,443	492,776	472,689	435,800	581,791	488,512	542,760	428,690	458,903	473,835	451,335	495,269	454,081	481,955	477,425	417,845	412,031	446,980
Maximum pores area S_{max} [µm^2]	5187.00	6078.00	5284.00	8427.00	7633.00	6917.00	7250.00	6405.00	9026.00	9904.00	45267.00	5751.00	8980.00	4961.00	9949.00	5712.00	25127.00	7713.00	10275.00	10751.00	17540.00	29960.00	7897.00	7587.00
Minimum pores area S_{min} [µm^2]	0.01	0.01	0.01	0.01	0.01	0.01	0.01	0.01	0.01	0.01	0.01	0.01	0.01	0.01	0.01	0.01	0.01	0.01	0.01	0.01	0.01	0.01	0.01	0.01
Average pores area S_{av} [µm^2]	0.73	1.12	0.84	0.61	0.70	1.10	0.62	1.06	0.80	0.66	1.39	0.88	0.55	0.66	0.94	0.65	0.71	1.58	0.67	0.76	0.54	0.46	0.52	0.72
Total pores perimeter P_t [µm] x 10^3	1,186,121	1,171,155	1,264,083	1,593,907	1,554,252	1,275,191	1,560,129	1,196,641	1,310,256	1,388,397	1,060,531	1,286,289	1,895,071	1,423,451	1,183,350	1,496,801	1,423,760	893,631	1,517,606	1,380,265	1,735,405	1,767,620	1,673,251	1,373,766
Maximum pores perimeter P_{max} [µm]	2350.00	3492.00	3444.00	4462.00	4204	2587	3990	3968	3177	5114	13396.00	2876.00	4748.00	2554.00	3508.00	2280.00	11934.00	2373.00	5020.00	3390.00	7698.00	14396.00	3796.00	2742.00
Minimum pores perimeter P_{min} [µm]	0.50	0.56	0.56	0.50	0.47	0.50	0.47	0.47	0.50	0.50	0.56	0.53	0.44	0.56	0.47	0.53	0.44	0.50	0.41	0.53	0.53	0.44	0.53	0.47
Average pores perimeter P_{av} [µm]	2.58	3.28	2.42	2.04	2.14	2.55	1.88	2.57	2.22	2.11	2.54	2.32	1.93	2.20	2.42	2.04	2.25	2.86	2.24	2.17	1.98	1.94	2.10	2.23
Maximum pores diameter D_{max} [µm]	81.27	87.97	82.02	103.58	98.58	93.85	96.08	90.31	107.20	112.30	240.07	85.57	106.93	79.48	112.55	85.28	178.87	99.10	114.38	117.00	149.44	195.31	100.27	98.29
Minimum pores diameter D_{min} [µm]	0.08	0.08	0.08	0.08	0.08	0.08	0.08	0.08	0.08	0.08	0.08	0.08	0.08	0.08	0.08	0.08	0.08	0.08	0.08	0.08	0.08	0.08	0.08	0.08
Average pores diameter D_{av} [µm]	0.31	0.39	0.27	0.23	0.24	0.29	0.24	0.30	0.25	0.25	0.31	0.27	0.23	0.27	0.28	0.24	0.28	0.32	0.27	0.24	0.22	0.23	0.25	0.26
Ultrapores [%]	0.3	0.2	0.2	0.4	0.3	0.2	0.3	0.2	0.2	0.3	0.1	0.2	0.3	0.3	0.2	0.3	0.2	0.1	0.3	0.2	0.4	0.4	0.3	0.3
Micropores [%]	46.1	36.5	29.2	27.0	25.3	22.4	23.9	23.7	19.7	25.9	16.0	19.8	21.4	31.8	18.6	22.4	25.3	14.4	30.8	19.5	23.3	28.1	33.7	23.9
Mezopores [%]	53.6	63.3	70.6	72.6	74.4	77.4	75.8	76.1	80.1	73.8	83.9	80.0	78.3	67.9	81.2	77.3	74.5	85.5	68.9	80.3	76.3	71.5	66.0	75.8
Average form index of pores K_{fav} [-]	0.474	0.491	0.500	0.493	0.503	0.497	0.522	0.499	0.489	0.519	0.487	0.483	0.478	0.49	0.50	0.49	0.51	0.49	0.505	0.511	0.500	0.498	0.512	0.485
Isometric pores [%]	19.0	18.0	21.1	16.3	17.6	17.2	25.8	18.6	15.7	23.0	19.1	13.8	13.9	17.1	23.7	18.3	21.6	20.5	19.0	20.8	18.7	18.2	23.6	16.1
Anisometric pores [%]	81.0	82.0	78.9	83.6	82.4	82.8	74.0	81.2	84.2	77.0	80.7	86.2	85.8	82.8	76.1	81.1	78.4	79.5	80.8	79.2	81.3	81.6	76.4	83.9
Fissure-like pores [%]	0.0	0.0	0.0	0.1	0.0	0.0	0.2	0.2	0.1	0.0	0.2	0.0	0.3	0.1	0.2	0.6	0.0	0.0	0.2	0.0	0.0	0.2	0.0	0.0
Microstructure anisotropy index K_a [%]	2.14	0.87	3.11	1.15	4.94	6.72	5.24	7.51	7.31	3.40	3.84	2.51	3.96	6.91	17.65	6.46	2.68	10.57	1.63	8.06	4.33	5.88	9.22	6.2
Dominant direction of pores α [°]	138	5	159	10	172	176	96	156	1	165	179	35	58	142	143	179	176	11	6	150	4	176	155	0
Specific surface area of pores [1/µm]	1.05	1.03	1.11	1.38	1.35	1.10	1.34	1.03	1.12	1.20	0.90	1.10	1.63	0.90	1.24	1.01	1.29	1.23	1.32	1.18	1.50	1.53	1.46	1.2

its deepest part (Table 4). In the Tomaszowice profile, the lowest value of this parameter is 383,409 μm^2, at the depth of 5.3–5.4 m. The highest value of this parameter, 542,027 μm^2, occurs at the depth of 1.2–1.3 m (Table 4).

In the Jastków profile, the maximum pores area (area of maximum pore) (S_{max}) ranges from 5,187 μm^2 in its shallowest part to 9,904 μm^2 in its deepest part. However, there is no clear trend in how the values of this parameter change with depth (Table 4). In the Stary Gaj profile, the lowest value of this parameter, 5,751.00 μm^2, occurs in the middle part of the profile, while the highest value, 45,267.00 μm^2, in the shallowest part. (Table 4). The maximum pores area shows great variation in the Piotrawin profile. The lowest value of this parameter is 4,961.00 μm^2, and it occurs in the shallowest part of the profile, while the highest value is 25,127.00 μm^2, nearly five times higher, and occurs at the depth of 3.2 m (Table 4). In the Tomaszowice profile, the values of the S_{max} parameter rise and fall alternately, ranging from 4,922.00 to 9,134.00 μm^2 (Table 4).

The minimum pores area (area of minimum pore) (S_{min}) reaches the same value of 0.01 μm^2 in the profiles of all sites (Table 4). In the Jastków profile, the average pores area (S_{av}) reaches the lowest value of 0.61 μm^2 at the depth of 210 cm, and the highest value of 1.12 μm^2 at the depth of 140 cm (Table 4). The value of this parameter shows a falling trend with increasing depth in the Stary Gaj profile. At the depth of 1.2–1.3 m, the value of this parameter is 1.39 μm^2, while at the depth of 3.6–3.7 m it reaches 0.55 μm^2 (Table 4). The average pores area shows great variation in the Piotrawin profile. After the initial increase of this parameter to 0.94 μm^2, it falls to 0.65 μm^2, and then rises again to 1.58 μm^2 (Table 4). The values of this parameter in the Tomaszowice profile range from 0.66 to 1.32 μm^2. The extreme values occur in the shallowest part of the profile, while the remainder of the profile has similar values of about 0.76 μm^2 (Table 4).

Perimeter of the pores

In the Jastków profile, the total pores perimeter (P_t) reaches the lowest values, about 1,170,000–1,180,000 μm, in the shallowest part, and the highest values, 1,593,907 and 1,554,252 μm, at the depth of 210–270 cm. In the Stary Gaj profile, the value of this parameter increases with depth, from 1,060,531 to 1,895,071 μm (Table 4). At the Piotrawin site, the values of total pores perimeter are similar across the entire profile and range from 1,183,350 to 1,496,801 μm, except for the lower part of the profile where the value is the lowest, 893,631 μm (Table 4). The total perimeter in the Tomaszowice profile has similar values ranging from 1,155,777 μm in the shallowest part of the profile to 1,460,268 μm in its middle part (Table 4).

In the Jastków profile, the maximum pores perimeter (P_{max}) increases from 2,350 μm at the depth of 95 cm to 4,462 μm at the depth of 210 cm. In the deeper part of the profile, the value of this parameter ranges from 2,587 μm at the depth

of 350 cm to 5,114 μm in the deepest part (Table 4). In the Stary Gaj profile, the maximum perimeter shows a very wide range of values. The highest value, 13,396.00 μm can observed in the shallowest part and is over four times higher than the lowest value (2,876.00 μm) in the middle part of the profile (Table 4). The values of this parameter in the Piotrawin profile are extremely varied. For a greater part of the profile, these values range from 2,280.00 to 3,508.00 μm. The biggest deviation was observed at the depth of 3.2 m where the parameter's value was 11,934.00 μm, nearly three times higher than the average value for the profile. In the Tomaszowice profile, the maximum perimeter does not show considerable variation and ranges from 2,048.00 μm at the depth of 6.8–6.9 m to 3,516.00 μm at the depth of 1.2–1.3 m (Table 4).

The values of the minimum pores perimeter (P_{min}) are in the range from 0.47 to 0.56 μm for the entire Jastków profile (Table 4). In the Stary Gaj profile, the values of this parameter decrease with increasing depth, but they do not show considerable variation, ranging from 0.56 to 0.44 μm (Table 4). In the Piotrawin profile, the minimum perimeter is 0.50 μm (+/–0.06) and it does not show any clear changing trend (Table 4). In the Tomaszowice profile, the minimum circumference has very similar values ranging from 0.47 to 0.56 μm (Table 4).

In the Jastków profile, the average pores perimeter (P_{av}) ranges from 1.88 to 3.28 μm. The highest values can be observed at the depth of 140 cm, and the lowest at the depth of 430 cm. (Table 4). In the Stary Gaj profile, the values of this parameter show a decreasing trend with increasing depth, in the 1.93–2.54 μm range (Table 4). In the Piotrawin profile, the average perimeter shows variation in the 2.00–3.00 μm range: it rises initially, then it falls, and then a growing trend is observed again (Table 4). In the Tomaszowice profile, the values of this parameter range from about 2 μm to nearly 3 μm, falling and rising alternately. Extreme values occur in the shallowest parts of the profile (Table 4).

Diameter of the pores

The maximum pores diameter (D_{max}) in the Jastków profile ranges from 81.2 to 112.3 μm, generally increasing with depth (Table 4). In the Tomaszowice profile, it changes from 115.4 to 64.2 μm with increasing depth (Table 4). In the Stary Gaj and Piotrawin profiles, this parameter ranges from 75.2 to 128.2 μm and from 79.48 to 178.8 μm respectively (Table 4). The minimum pores diameter (D_{min}) does not change in the profiles under study and has the value of 0.08 μm (Table 4). The average pores diameter (D_{av}) ranges from 0.39 to 0.25 μm in the Jastków profile, reaching the lowest values in its deepest part (Table 4). In the Tomaszowice profile, the average diameter is in the 0.22–0.27 μm range; initially it falls, but then it grows with increasing depth (Table 4). In the Stary Gaj profile, the average diameter decreases with depth from 0.31 to 0.23 μm (Table 4). In the Piotrawin profile, the average diameter generally increases with depth from 0.27 to 0.32 μm (Table 4).

Size of the pores

The share of ultrapores (no more than 0.1 μm) is similar, and ranges from 0.2 to 0.3% in the Jastków profile, from 0.2 to 0.4% in the Tomaszowice profile, from 0.1 to 0.3% in the Stary Gaj profile, and from 0.1 to 0.3% in the Piotrawin profile (Table 4). The share of micropores (10 μm <Ø<1,000 μm) ranges from 19.7 to 46.1% in the Jastków profiles, decreasing with increasing depth (Table 4). In the Tomaszowice profile, it ranges from 19.5% to 33.7% (Table 4). In the Stary Gaj profile, the value of this parameter increases with depth from 16.0 to 21.4%, while in the Piotrawin profile it generally decreases with depth from 31.8 to 14.4%. (Table 4). The percentage share of mesopores (0.1 μm <Ø<10 μm) is varied, and ranges from 53.6 to 80.1% in the Jastków profile, increasing with depth (Table 4). In the Piotrawin profile, it decreases with depth from 83.9 to 78.3% (Table 4). In the Tomaszowice profile, the share of mesopores ranges from 68.9 to 80.3%, while in the Stary Gaj profile from 46.6 to 70.1% (Table 4).

The pore form coefficient

The average form index of pores (K_{fav}) reaches relatively low values, ranging from 0.47 to 0.51 in the Jastków profile (increasing with depth), from 0.48 to 0.51 in the Tomaszowice profile, from 0.47 to 0.48 in the Stary Gaj profile, and from 0.49 to 0.51 in the Piotrawin profile (Table 4).

Shape of the pores

The number of isometric pores in the Jastków profile ranges from 15.7 to 23.0% in its deepest part, from 19.1 to 13.8% in the Stary Gaj profile (decreasing with depth), in the Piotrawin profile from 17.1 to 23.7%, and in the Tomaszowice profile from 16.0 to 23.6% (Table 4). Anisometric pores have the largest share in all profiles under study: from 74.0 to 84.2% (Jastków profile), from 76.4 to 83.9% (Tomaszowice profile), from 80.7 to 86.1% (Stary Gaj profile), and from 76.0 to 82.8% (Piotrawin profile) (Table 4). Their share varies depending on the depth. Interstitial pores account for only 0.1–0.2% (Jastków profile), 0.2% (Tomaszowice profile), 0.2–0.3% (Stary Gaj profile), and 0.3–0.6% (Piotrawin profile). Their share varies depending on the depth (Table 4).

Microstructure anisotropy index

The microstructure anisotropy index (K_a) ranges from 0.87 to 7.5% in the Jastków profile, and from 1.6 to 9.2% in the Tomaszowice profile (Table 4). In the Stary Gaj and Piotrawin profiles, the values of this index range from 2.5 to 3.9% and from 2.6 to 17.6%, respectively (Table 4).

Orientation of structural elements

In the Jastków profile, the dominant direction of pores (α) reaches quite extreme values: from 1° to 176° (Table 4). Large differences are observed for this parameter in the Stary Gaj profile as well. This parameter reaches its minimum value (35°) in the middle part of the profile, and the highest value (179°) in its shallowest part (Table 4). The orientation is similar across the entire Piotrawin profile, and ranges from 142 to 179° (Table 4). In the Tomaszowice profile, the lowest value of orientation (116°) occurs in its shallowest part, while in the remaining part of the profile it ranges from 142 to 164° (Table 4).

Specific surface area of the pores

The specific surface area in the Jastków profile ranges from 1.03 1/μm at the depth of 140 cm and 480 cm to 1.38 1/μm at the depth of 210 cm (Table 4). The values of this parameter in the Stary Gaj profile range from 0.90 to 1.63 μm^2, increasing with depth (Table 4). In the Piotrawin profile, specific surface area is characterised by considerable variation: from 0.76 1/μm in the lowest part of the profile to 1.29 1/μm in its middle part (Table 4). In the Tomaszowice profile, the value of this parameter does not vary significantly, staying in the 0.99–1.27 1/μm range (Table 4).

5. DISCUSSION

5.1. Comparison of grain-size distribution and microstructure of loess forming the bottoms and slopes of depressions

The loess cover in the studied closed depressions has grain-size distribution characteristics typical of younger upper loess documented in numerous profiles in the Nałęczów Plateau (Harasimiuk 1987, Maruszczak 1991, Harasimiuk and Jezierski 2000).

The grain-size distribution characteristics of loess forming the bottoms and slopes of depressions show slight differences. The loess under the bottoms of the CDs are characterised by the greater variation of clay fraction content depending on depth in relation to the loess in the slopes of the CDs. The variation reaches 3–5% in the individual depressions. The biggest variations, i.e. 5%, were found in the Jastków and Piotrawin profiles (Table 2, Fig. 2). The loess in the slopes of the CDs shows the smallest variations of clay fraction content: only 1.5–3% in the individual forms. The biggest variations, i.e. 3%, occur in the Jastków and profile (Table 2, Fig. 2). The obtained results correspond with the results of a small number of previously conducted studies presenting the

variation of loess grain-size distribution characteristics in relation to micro-relief forms in the loess cover (Maruszczak 1954, Czarnecki and Solnceva 1992)

Similarities were found between the younger upper loess characteristics determined by Grabowska-Olszewska (1988) and the microstructure of younger upper loess in the slopes of the CDs under study. Carbonate loess in the slopes has primary skeletal microstructure or loosely packed microstructure. In the deeper parts (deeper than 3 m), the loess in most profiles (except Jastków) has primary skeletal microstructure with preserved synsedimentary characteristics of the aeolian environment (horizontal laminae of the clay and silt fraction). Clear differences occur in the microstructure of the loess forming the bottoms and slopes of the CDs (Fig. 3). The loess under the bottoms of the CDs are mainly characterised by matrix microstructure with a medium and high degree of packing, increasing with depth. On the slopes, loosely or medium packed matrix microstructure occurs only in the topmost parts of the profiles, within decalcified loess.

Differences also occur in the pore space (Table 3, 4, Fig. 4). The loess in the bottoms of the CDs has a greater share of micropores (20–53%) in comparison with the slopes (14–46%), and a smaller share of mesopores (46–80% compared to 46–84% on the slopes). In the bottoms of the CDs, larger micropores became "closed", and the matrix microstructure became densely packed (Fig. 3). The smallest micropores with a diameter reaching 1–2 μm are the most numerous. On the slopes, larger micropores were found to be only partially closed. Besides, the presence of large micropores and smaller mesopores was also found. The loess in the bottoms of the CDs have a slightly lower porosity (30–45.7%) in comparison with the slopes (30–48%), and greater average diameter of the pores (0.24–0.46 in comparison with 0.22–0.39 on the slopes) (Table 3, 4). The structural elements are mostly anisometric both beneath the bottoms and on the slopes of the depressions because the average form index of pores (K_{fav}) has a similar value of 0.4–0.5 (Table 3, 4, Fig. 4). The number of anisometric pores shows a greater variation in the profiles under the bottoms of the CDs, reaching 86.6%, i.e. up to 2% more than on the slopes (Table 3, 4, Fig. 4). The microstructure anisotropy index (K_a) reaches higher values in the loess forming the bottoms rather than the slopes of the depressions (3.1–18.4%) (Table 3, 4, Fig. 4). Micropores in the bottoms of the depressions were transformed from isometric shape in the upper part of the profiles to more anisometric shape in the deeper parts.

At various depths of some depressions (2 m in Stary Gaj, 4.6 m in Jastków, 5.2 m in Tomaszowice), loess with skeletal microstructure typical of loess forming the slopes of the CDs was found amidst loess with matrix microstructure. This can be indicative of the movement of loess packages due to slides from the slopes of the CDs, or of the spatially varied impact of water (filtration channels) within the thick loess cover.

5.2. Record of diagenetic processes and assessment of the morphological effects of their impact

The variation of the clay fraction content as well as the size and shape of the pores (share of micro- and mesopores) as well as the orientation of clay microaggregates can indicate the migration of clay matter in the loess under the influence of the water infiltration (mechanical suffosion *sensu* Maruszczak 1954). According to Afelt (2013), the selective migration of clay particles through interskeletal pores occurs during mechanical suffosion with a filtration stream. This process leads to a change in the pore space configuration with regard to micro- and mesopores and ordering of the pore space. Stronger variations of clay fraction content in the loess forming the bottoms of the CDs indicate a stronger movement of this fraction in the vertical profile beneath the bottoms of the CDs in comparison with their slopes. The movement of clay particles was accompanied by their partial deposition in some horizons, influencing the variation of clay fraction content depending on depth, as documented in the profiles under study.

The movement of the clay fraction in the studied profiles also contributed to the infilling of the pore space (also space remaining after the leached $CaCO_3$) and the closing of micropores. This caused a reduction of loess porosity in the bottoms of the depressions. The vertical migration of the finest material caused an increase in the degree of its packing leading to the formation of the matrix microstructure that dominates in the bottoms of the CDs.

The upper parts of the analysed profiles, both in the bottoms and on the slopes of the CDs, are enriched with the clay fraction. This enrichment can be linked to the impact of pedogenetic processes (illuviation accompanying the development of Luvisols). The range of pedogenic enrichment in the clay fraction is greater in the bottoms of the CDs, reaching the depth of more than 2 m, while on the slopes it reaches the depth of only about 1 m. In the deeper parts of the profiles (deeper than 2.5 m), the clay fraction content evens out, reaching about 6–9% in the bottoms and 5–7% on the slopes.

The presence of matrix microstructure with a considerable degree of packing, the higher, but decreasing with the depth, share of anisometric pores, and the higher value of the anisotropy index in the loess forming the bottoms of the CDs can indicate subsidence, to which loess in the bottoms of the CDs were more susceptible. This is also confirmed by decreasing with the depth of such parameters as: number of pores, total and maximum pores area, maximum perimeter and diameter of the pores.

Hydroconsolidation, also described as filtration consolidation (Liszkowski 1971), is a typical process to which loess is subjected due to calcium carbonate and clay matter content (Rogers *et al*. 1994, Smalley *et al*. 2006, Smalley and Markowic 2014). Hydroconsolidation is defined as the destruction of loess microstructure under the influence of water, resulting in the slumping of

loess (Rogers *et al*. 1994). Changes of this type have been documented in loess profiles by many researchers (Liszkowski 1971, Grabowska-Olszewska 1988, Frankowski and Grabowski 2006). The loess forming the bottoms of the CDs is decalcified, while the loess forming the slopes contain 10% of $CaCO_3$. Given the documented small difference in clay fraction content in the loess forming the bottoms and slopes of the CDs under study, it seems that changes in microstructure and, in consequence, the quantitative (morphological) effect of loess subsidence in the bottoms of the depressions were strongly influenced by $CaCO_3$ leaching (chemical suffosion *sensu* Maruszczak 1954). Studies by Grabowska-Olszewska (1988) suggest that, after the leaching of $CaCO_3$ that creates cementation contacts between mineral grains, the loess is more water-resistant. According to Liszkowski (1971), although mechanical erosion is widespread in loess areas, the relief-forming role of this process is minimal because the leaching of clay particles is accompanied by their accumulation in the pore space of the ground mass. This is confirmed by the obtained investigation results showing that strong depth-dependent variation of clay fraction content is characteristic in the bottoms of the depressions below the range of pedogenesis. This suggests the multi-stage migration of the clay fraction and makes it difficult to obtain a quantitative assessment of the morphological effect of this process.

Taking into account the average calcium carbonate and clay fraction content in the unchanged loess forming the slopes of the closed depressions, we can estimate the potential maximum subsidence (slumping) of land as a result of the total leaching of $CaCO_3$ and the clay fraction (Table 5).

Table 5. Potential morphological effect of hydroconsolidation and suffosion in the loess forming the CDs

Index	Jastków	Stary Gaj	Piotrawin	Tomaszowice
Depth of the present CDs: Wg (cm)	70	490	250	340
Thickness of colluvia: C (cm)	120	80	100	0
Depth of the primary CDs: Pg (cm); Pg = Wg – C	190	570	350	340
Average porosity of carbonate loess forming the slopes of the CDs (%)	39.49	45.34	39.03	38.12
Potential subsidence index for the bottom of the initial CDs due to the destruction of pores: P (cm)	39.49	45.34	39.03	38.12
Potential subsidence index for the bottom of the initial CDs due to $CaCO_3$ leaching: Cca (cm)	10	10	10	10
Average clay fraction content in the loess forming the slopes of the CDs: Y	6.68	5.0	5.93	4.92
Potential subsidence index for the bottom of the initial CDs due to clay fraction leaching (cm)	6.68	5.0	5.93	4.92
Potential maximum subsidence index for the bottom of the initial CDs: Ws (cm); Ws = P + Cca + Y	56.18	60.34	54.96	53.04
Depth of the initial CDs: Ig (cm); Ig = Pg – Ws	133.82	509.66	295.04	286.96

The potential maximum subsidence in individual CDs is: 16.68 cm, 15 cm, 15.93 cm, 14.92 cm. If microstructure changes consisted of the total reduction of pores in the loess, the studied CDs would become deeper by 38–45 cm (Table 5). The maximum subsidence (slumping) of land, resulting from the total leaching of the clay fraction and $CaCO_3$ and removal of pores would amount to 56.18 cm (Jastków), 60.34 cm (Stary Gaj), 54.96 cm (Piotrawin), and 53.04 cm (Tomaszowice) (Table 5). This value should be construed as the potential (maximum) morphological effect related to hydroconsolidation and suffosion (maximum subsidence of the bottom of a CD). However, the calculated value is considerably inflated, and the actual value is difficult to estimate. Nonetheless, it will not exceed the maximum value provided above. The original depth of the CDs under study (Table 5) is several times greater than this potential morphological effect of hydroconsolidation and suffosion; hence they would not lead to the formation of the depressions under study. The investigations suggest that mechanical suffosion (*sensu* Maruszczak 1954) recorded beneath the bottoms of the depressions is a secondary process developing within initial depressions formed previously as a result of primary morphogenetic processes (e.g. thermokarst or deflation processes). The leaching of $CaCO_3$ (chemical suffusion *sensu* Maruszczak 1954) probably began and/or could accompany the final phase of younger upper loess deposition during the thawing of various forms of ground ice (Kołodyńska-Gawrysiak *et al*. 2018).

6. CONCLUSIONS

The qualitative and quantitative characteristics of the microstructure and grain-size distribution of the loess forming the bottoms of CDs indicate the impact of syn- and post-depositional diagenetic processes related to the leaching of $CaCO_3$, migration of the clay fraction, and hydroconsolidation under the influence of the water infiltration into the loess cover.

Different degrees of the development of these processes were recorded in the bottoms and slopes of the CDs. The greater changes in microstructure as well as clay fraction and $CaCO_3$ content occurred in the loess under the bottoms of the CDs. The microstructure of carbonate loess did not change on the slopes of the CDs, below the range of pedogenesis. The morphological effect of loess diagenesis under water infiltration was manifested in the deepening of the initial CDs formed previously under the influence of primary morphogenetic processes.

ACKNOWLEDGEMENTS

The research was financially supported by the National Science Centre Grant 2012/07/B/ST10/04164, PB-B-12-287-00-13: “The origin and evolution

of closed depressions in the loess areas in the Lublin Upland and their importance for the reconstruction of postglacial morphogenesis of the loess cover".

REFERENCES

[1] Afelt, A., 2013. *The* impact *of* loess transformation *on its* filtration characteristics. Biuletyn PIG, 456: 27–32 (in Polish).

[2] Antoine, P., Rousseau, D.-D., Degeai, J.-P., Moine, O., Lagroix, F., Kreutzer, S., Fuchs, M., Hatté, Ch., Gauthier, C., Svoboda, J., Lisá, L., 2013. *High-resolution record of the environmental response to climatic variations during the Last Interglacial-Glacial cycle in Central Europe: the loess-palaeosol sequence of Dolní Vestonice (Czech Republic)*. Quaternary Science Reviews, 64: 17–38.

[3] Czarnecki, R., Solnceva, N.P., 1992. *Drainage basins of Sandomierz area (part II)*. Przegląd Geograficzny, LXIII(1–2): 143–149 (in Polish).

[4] Gillott, J.E., 1987. *Clay in Engineering Geology*. Elsevier, Amsterdam–New York.

[5] Grabowska-Olszewska, B., Osipov, V.I., Sokolov, V.N., 1984. *Atlas of the Microstructure of Clay Soil*. Państwowe Wydawnictwo Naukowe, Warszawa.

[6] Grabowska-Olszewska, B., 1988. *Engineering-geological problems of loess in Poland*. Engineering Geology, 25.

[7] Grabowska-Olszewska, B., 1998. *Collapse settlement*. In: B. Grabowska-Olszewska (ed.) Properties of Unsaturated Soils. Wydawnictwo Naukowe PWN, Warszawa (in Polish).

[8] Harasimiuk, M., 1987. *Lithologic properties as indices of the sedimentation conditions of the Vistulian loesses in the eastern part of the Nałęczów Plateau (SE Poland)*. Annales UMCS, sec. B, 41(11): 179–202.

[9] Harasimiuk, M., Henkiel, A., 1976. *Peculiarities of the loess cover in the western part of the Nałęczów Plateau*. Biuletyn PIG, 297: 177–181.

[10] Harasimiuk, M., Jezierski W., 2001. *Loess profile in Skowieszyn in Lublin Upland.* In: H. Maruszczak (ed.), Basic Loess Profiles in Poland. Wydawnictwo UMCS, Lublin, pp. 93–100 (in Polish).

[11] Frankowski, Z., Grabowski D., 2006. *Engineering-geological and geomorphological conditions of gully erosion in loess deposits in the Kazimierz Dolny area (Opolska Droga Gully)*. Przegląd Geologiczny, 54 (9): 777–783 (in Polish).

[12] Kołodyńska-Gawrysiak, R., Chabudziński, Ł. 2012. *Morphometric features and distribution of closed depressions on the Nałęczów Plateau (Lublin Upland, SE Poland)*. Annales UMCS, sec. B, LXVII(1): 45–61.

[13] Kołodyńska-Gawrysiak, R., Harasimiuk, M., Chabudziński, Ł., Jezierski, W., 2018. *The importance of geological conditions for the formation of past thermokarst closed depressions in the loess areas of Eastern Poland*. Geological Quarterly, 62(3): 685–704.

[14] Liszkowski, J., 1971. *Filter deformations of loess deposits*. Biul. Geol. UW, 13: 87–126.

[15] Maruszczak, H., 1954. *Sinkholes in less areas of Lublin Upland*. Annales UMCS, sec. B, VIII: 123–237 (in Polish).

[16] Maruszczak H (ed.), 1991. *Main Sections of Loesses in Poland*. Lublin, 200 p.

[17] Mitchell, J.K., 1993. *Fundamentals of Soil Behavior*. John Wiley & Sons, Inc., New York–Chichester–Brisbane–Toronto–Singapore.

[18] Osipov, V.I., Sokolov, V.N., Eremeev, V.V., 2004. *Clay Seals of Oil and Gas Deposits*. A.A. Balkema Publishers, Netherlands.

[19] Rogers, C.D.F., Dijkstra, T.A., Smalley, I.J., 1994. *Hydroconsolidation and subsidence of loess: Studies from China, Russia, North America and Europe.* Engineering Geology, 37: 83–113.

[20] Sergeyev, Y.M., Grabowska-Olszewska, B., Osipov, V.I., Sokolov, V.N., Kolomenski, Y.N., 1980. *The classification of microstructures of clay soil*. Journal of Microscopy, 120: 237–260.

[21] Smalley, I.J., Mavlyanova, N.G., Rakhmatullaev, Kh.L., Shermatov, M.Sh., Machalett, B., O' Hara Dhand, K., Jefferson, I.F., 2006. *The formation of loess deposits in the Tashkent region and parts of Central Asia; and problems with irrigation, hydrocollapse and soil erosion*. Quaternary International, 152–153: 59–69.

[22] Smalley, I.J., Markovic, S.B., 2014. *Loessification and hydroconsolidation: There is a connection*. CATENA, 117: 94–99.

[23] Smart, P., Tovey K., 1982. *Electronomicroscopy of Soils and Sediments: Techniques*. Clarendom Press, Oxford.

[24] Soil Taxonomy, 1975. *Soil Conservation Service U.S. Department of Agriculture*. Handbook, no. 436, 754 pp.

[25] Sokolov, V.N., Yurkovets, D.I., Razgulina, O.V., 2002. *Stiman (Structural Image Analysis): A software for quantitative morphological analysis of structures by their images (User's manual. Version 2.0)*. Laboratory of Electron Microscopy, Moscow State University, Moscow, pp. 75.

[26] Tovey, N.K., Wong, K.Y., 1973. *The preparation of soils and other geological materials for the scanning electron microscope*. Proceedings of the International Symposium on Soil Structure, Gothenburg, Sweden, pp. 176–183.

[27] Trzciński, J., 2004. *Combined SEM and computerized image analysis of clay soils microstructure: technique & application*. In: R.J. Jardine, D.M. Potts, K.G. Higgins (eds.), Advances in Geotechnical Engineering. The Skempton conference. Thomas Telford, London, pp. 654–666.

[28] Trzciński, J., 2008. *Microstructure and physico-mechanical properties of tills in Poland*. Geologija – Vilnus 50, Supplement, 26–39.